EEET ECOLOGICAL ENGINEERING & ENVIRONMENTAL TECHNOLOGY

Ecological Engineering & Environmental Technology 2023, 24(8), 181–193
https://doi.org/10.12912/27197050/171494
ISSN 2719–7050, License CC-BY 4.0

Received: 2023.07.27
Accepted: 2023.09.25
Published: 2023.10.10

Removal of Dyes by Adsorption Process Using Date Pits as Material Environmentally Friendly

Abderrazzak Adachi[1*], Faiçal El Ouadrhiri[1], Ibtissam El Manssouri[2], Fatima Moussaoui[1], Soukaina El Bourachdi[1], Amal Lahkimi[1]

[1] Laboratory of Engineering, Molecular Organic Materials and Environment, Faculty of Sciences Dhar El Mahraz University Sidi Mohamed Ben Abdallah, Fez 30000, Morocco

[2] Laboratory of Biotechnology of Environment, Agroalimentary, Health, University Sidi Mohamed Ben Abdelah, Faculty of Sciences, Fez 30000, Morocco

* Corresponding author's e-mail: abderrazzak.adachi@usmba.ac.ma

ABSTRACT

This study is based on the use of a natural material in the adsorption process to remove organic pollutants. The objective is to assess its effectiveness in adsorbing the organic pollutant MB from an aqueous solution, while operating in an open system. The DP bioadsorbent was characterized using FTIR and SEM. To determine their effect on adsorption efficiency, a number of variables were examined, including contact time, concentration of pollutant MB, adsorbent mass, pH, temperature, and adsorbent particle size. The effect of these variables on adsorption efficiency shows that a removal rate of 92.66% is achieved under optimum conditions, including a contact time of 35 minutes, a concentration of pollutant MB of 22.5 $mg \cdot l^{-1}$, an adsorbent mass (m_{DP}) of 1.1 $g \cdot l^{-1}$ and a solution pH of 5.6. In addition, a progressive decrease in adsorption efficiency is observed with increasing temperature and adsorbent mass. On the other hand, this efficiency increases with increasing a concentration of pollutant MB. Three popular models, the Freundlich, Langmuir, and Dubin-Radushkevich models, have been used to examine the adsorption isotherms of the MB dye on DP. With a correlation factor of 0.98, it was discovered that MB adsorption monitored by the Freundlich isotherm. The Langmuir and Dubinin-Radushkevich models, however, do not adequately describe the data. The kinetic results were studied using the pseudo-first-order and pseudo-second-order equations, and show that MB dye adsorption on DP (adsorbent) follows the pseudo-second-order model. Also estimated were thermodynamic parameters such as (ΔH°), (ΔS°), (ΔG°), enthalpy, entropy, Gibbs free energy respectively to anticipate the character of adsorption. The results indicate that the adsorption process of MB on the bioadsorbent is exothermic. The results derived from the ΔG° values lead to the conclusion that the adsorption of MB occurs spontaneously.

Keywords: adsorption, BM, natural adsorbent, DP, isotherm, open system, kinetics, thermodynamics.

INTRODUCTION

The term "pollution" refers to the degradation of the environment brought on by artificial substances, which has resulted in the extinction of numerous animal and plant species as well as the rise of new phenomena that are damaging to human health, such as climate change (Al-Ghouti et al., 2010). In addition to impacting the air and soil, this pollution also has a significant impact on a considerable portion of the water. Various industrial sectors, including textiles, paper, leather, food, and cosmetics, utilize colorants extensively (Ait Hmeid, 2021). These industries also use a tremendous amount of water. Once discharged, these colors seriously harm human health by having mutagenic and cancerous consequences (Alakhras et al., 2020; Alipour et al., 2021), various modifications to the aquatic environment (Adachi et al., 2023) if they are released into the environment without being properly treated or with inadequate treatment (Ahmad et

al., 2019). Several methods for treating dye-laden effluents have been developed and tested in order to lessen the effects of this pollution. These include biological processes (Ledakowicz et al., 2001), coagulation/flocculation (Zhou et al., 2014), photo degradation (Diarra, 2019), ozonation (Soares et al., 2006), oxidation (Adachi et al., 2022), separation through membranes (Tan et al., 2015; Alasadi, 2019). Adsorption is thought to be one of the most successful techniques that has been used to successfully remove colors from wastewater (Abdallah et al., 2016) Because it is inexpensive and easily accessible. The facility to easily eliminate dyes from Water solutions by means of various materials, in particularly activated carbon (Miyah et al., 2015), has been the subject of extensive research (Douara et al., 2016; Susanti et al., 2019). In recent times, a variety of adsorbents have been developed for the purpose of eliminating of dyes (Zhang et al., 2016). Examples of such materials include: clay (Awasthi et al., 2019), double hydroxides in layers (Shan et al., 2015), steel oxides (Chakma and Moholkar, 2016), changed-nature goethite (Ouachtak et al., 2020), sedimentary materials (Dra et al., 2019). Activated carbon is an incredibly expensive product. It is therefore exciting to look for an adsorbent that is less expensive, more effective, and natural (Arami et al., 2005). Alternative materials for dye adsorbents have been suggested, including bio-materials. Date pits in particular have drawn a lot of interest because of their advantages, including affordability, availability, and environmental safety. Date pit fruit (DP) consists of seeds and a pulpy pericarp. A byproduct of many date processing plants, date palm seeds are used to make pitted dates, date powder, date syrup, date juice, chocolate-covered dates, and date confections (Rahman et al., 2007). Date palm pits are also numerous and widely dispersed, which makes them attractive environmental adsorbents that can be used in industrial operations (Saad et al., 2008). In a study, Javid et al. used modified carbonized DP with ZnO nanoparticles to remove bisphenol A and nonylphenol from aqueous solutions, Under optimal conditions, they discovered that the maximum removal efficiency was 95% (Javid and Malakootian, 2017; Javid et al., 2019). Nevertheless, the thorough investigation of date pits' ability to adsorb BM dye has not yet been conducted (Arami et al., 2005). Therefore, the aim of this work is to use a variety of techniques, including SEM and FTIR, to assess the physical and chemical characteristics of bioadsorbent. The effectiveness of employing date pits as an economical and environmentally acceptable natural bio adsorbent to remove MB dyes from aqueous media will then be assessed. The effects of contact time, initially MB concentration, bioadsorbent mass (DP), solution pH, temperature (T), and DP particle size on the MB adsorption process on the bioadsorbent were also studied.

MATERIALS AND METHODS

PREPARATION OF A BIOADSORBENT

De-pitted (DP) Moroccan dates had their pits recovered, separated, and rinsed to get rid of any contaminants. They were then baked for 24 hours at 110°C to dry them out (Ali et al., 2022). Subsequently, the bio adsorbent was ground in a grinder and sieved to obtain particles of the same size with diameters of 40, 63, 125, and 200 μm (Fig. 1). The pits of dates consist of approximately hemicellulose, lignin, cellulose, and carbohydrates (Pal et al., 2021; Bouchelta et al., 2008).

Adsorbate

The dye investigated in the research is Methylene Blue (MB) of analytical-grade, which was obtained from Sigma-Aldrich. Its chemical formula is provided, and the Table 1 presents the discussed maximum absorption wavelength. The principal drawbacks of dye (MB) in textile wastewater are its non-biodegradability, its high visibility due to its bright color even at extremely low dye concentrations (1 $mg \cdot L^{-1}$), and its high toxicity, which makes it difficult to remove using conventional procedures (Bayomie et al., 2020).

Adsorption study

For this study, a sample solution was created from the BM dye. In a batch system with continuous stirring, the adsorption study was carried out using 1 g of date pits (DP) combined with the BM solution at room temperature (Fig. 2). To investigate the kinetic adsorption, the concentration was determined using a UV-visible spectrophotometer (VR, 2000) at a wavelength of 665 nm. Every five minutes, several samples were obtained. The sample was then centrifuged to separate the bioadsorbent (DP) from the MB liquid. During the adsorption experiment, the pH of the solution was

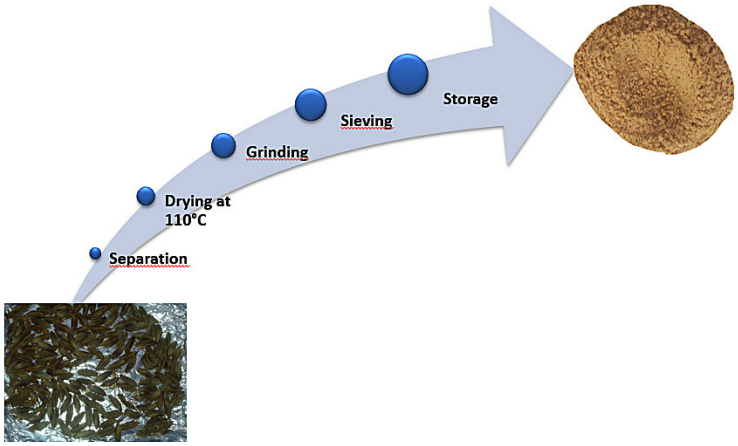

Fig. 1. Illustration of date pits adsorbent preparation.

adjusted using 0.2 M hydrochloric acid (HCl) and 0.2 M sodium hydroxide (NaOH) from Sigma-Aldrich. BM dye removal efficiency was calculated using the following formula (El Ouadrhiri et al., 2023):

$$\text{Removal } (\%\ R) = \left(\frac{C_0 - C_t}{c_0}\right) \cdot 100 \quad (1)$$

where: C_0 and C_t represent, respectively, residual MB concentrations at t = 0 and t ≠0.

The following equation was used to determine the date pits' capacity to adsorb MB dye (Narasimharao et al., 2022):

$$q_e = \left(\frac{C_0 - C_e}{m}\right) \cdot V \quad (2)$$

In this context, q_e (mg. g^{-1}) corresponds to the equilibrium adsorption capacity, C_0 (mg. L^{-1}) indicates the concentration of Dye (MB) at t=0, C_e (mg·L^{-1}) is the concentration of MB dye at equilibrium. V (L) denotes the volume of the MB solution, m (g) represents the mass of DP.

The techniques for characterization

To determine the composition and morphology of the bioadsorbent (DP), we used Fourier transform infrared spectroscopy (FTIR, vertex 70) and scanning electron microscopy (SEM, quanta 200).

RESULTS AND DISCUSSIONS

Characterization of FTIR

Figure 3 displays the infrared spectra (500–4000 cm^{-1}) of the powdered date pits. The chemical analysis of the DP powder reveals wide bands in the range of 3650–3000 cm^{-1}, attributed to the stretching of O-H bonds (Wang et al., 2016). The C-H stretching vibrations of $-CH_3$ and $-CH_2$ could be responsible for the peaks seen at 2928, 2850 cm^{-1}, respectively. The presence of proteins in the date wells can be verified by the picks observed at 1643 and 1545 cm^{-1}, which are attributed to Amide I and Amide II respectively (Yuvaraja et al., 2020). The existence the alcohol is confirmed by the strong band at 1400 cm^{-1}, which represents the vibration of C-H deformation, the band at 1605 cm^{-1}, which corresponds with O-H in the plane, and the band at 1000 cm^{-1} (Dutta, 2017). Analysis of this graph indicates that the material under study is primarily composed of carbon, hydrogen, and oxygen atoms, suggesting it to be an organic compound.

Characterization of SEM

SEM was utilized to visualize the texture and morphology of the natural adsorbent of DP in its raw state 4(a), 4(b), and after conducting the BM adsorption tests 4(c), 4(d). The figure below 4(a), 4(b) shows that our material has a smooth and

Table 1. Adsorbate characteristics

Organic pollutant	Molecular formula	Molecular mass (g/mol)	Maximum length (nm)	Category
Methylene blue	$C_{16}H_{18}ClN_3S$	319,85	665	Cationic dye

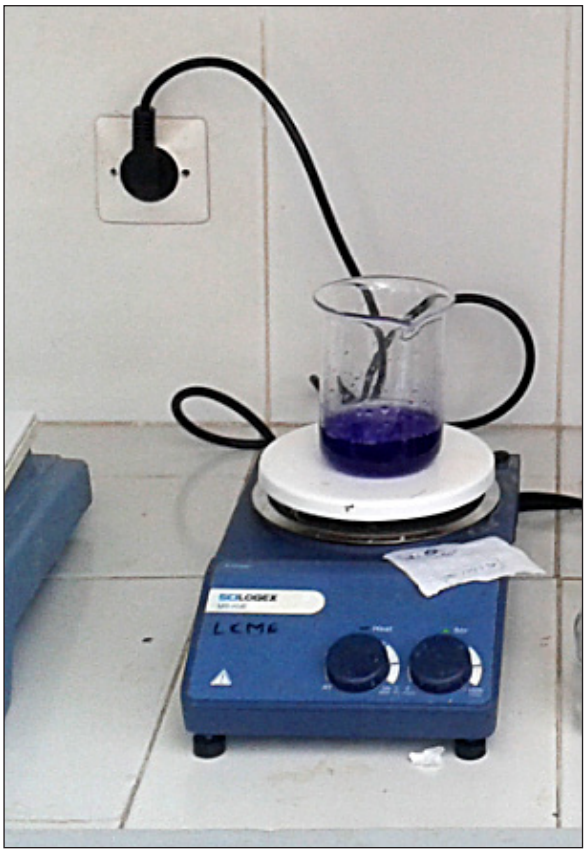

Fig. 2. Experimental equipment utilized in the adsorption procedure

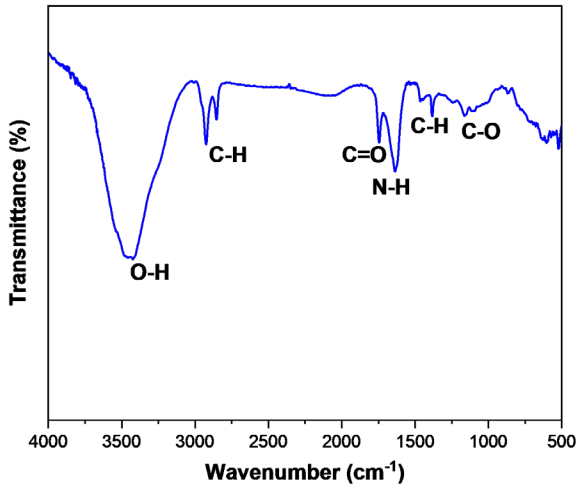

Fig. 3. Infrared spectrum of the DP bioadsorbent

porous structure, indicating a good potential for trapping and adsorbing the BM dye on the surface of the adsorbent (date pits) (Hassan et al., 2020). However, after BM adsorption on the date pits, SEM observation reveals that the surface of the BM-loaded material appears rugged and striated due to pore surface coverage by adsorbed BM dye molecules in figures 4(c) and 4(d). This finding suggests that date pits might work well as a bio-adsorbent to remove dangerous dyes from wastewater.

Study of different parameters on elimination rates effect of contact time

The influence of contact time improves the kinetic performance of adsorption between the adsorbent and the adsorbate as well as the equilibrium adsorption of pollutants (Gómez et al., 2007). The results of evaluating the BM adsorption by date pits at various time intervals are shown in Figure 5. As illustrated in Figure 5, during initial 35 minutes of the experiment, the concentration of BM adsorbed on the material increases with time, which perhaps be attributed to the availability of activated surfaces on the bioadsorbent (Yang, 2011). From 35 to 55 minutes, no significant change in the concentration of BM is observed. The results indicate that adsorption equilibrium is reached after only 35 minutes with a capacity of 14.56 mg/g. Perhaps equilibrium is reached after the majority of sites are occupied by the organic pollutants of BM (Li et al., 2009). For further experiments, it is recommended to fix the contact duration at 35 minutes, which is considered the optimal time.

Effect of MB concentration

According to the curves in Figure 6, a quick accretion of capacity is generally observed at low concentrations, and this capacity continues to increase with higher initial concentrations of MB (Ahmad et al., 2022). This is due to the high affinity between the exchange bioadsorbent and dye. A saturation plateau then appears, indicating saturation of the active sites on the adsorbent material. In summary, adsorption efficiency increases from 5.88 mg. g^{-1} to 24.63 mg·g^{-1} as the concentration of MB organic pollutants rises from 15 mg·L^{-1} to 35 mg·L^{-1}. Figure 7 shows the variations of adsorption capacity and removal efficiency with MB dye concentrations. The two trajectories are observed to cross at a location that corresponds to the optimal concentration (Pandian et al., 2015). The optimum initial concentration of the MB solution was determined to be 22.5 mg·L^{-1} based on the results. This concentration achieved a decolorization rate of approximately 91% with an adsorption efficiency of 21 mg·g^{-1}.

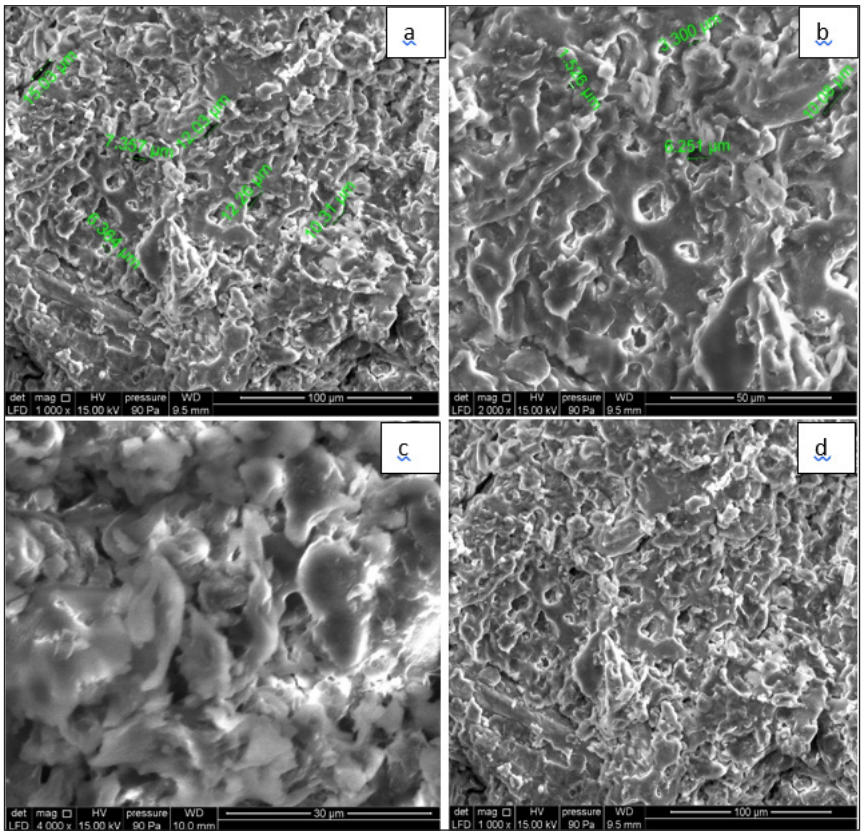

Fig. 4. Microscopic imaging of adsorbent in its raw state (a),(b), adsorbent in the case of BM adsorption (c),(d)

Effect of m_{DP}

The proportion of bioadsorbent applied plays a crucial role in the adsorption procedure, as this directly affects the efficiency of dye removal (Xing et al., 2023). Figure 8 shows variations in adsorption capacity (qe) and discoloration rate (%R) depending on bioadsorbent mass (DP). The results demonstrate that increasing the mass of date pit adsorbent from 0.5 to 2.5 g results in an increase in the decolorization rate from 86.22% to 89.65% for organic MB pollutants (Adachi et al., 2023). Conversely, there is a decrease in adsorption efficiency, decreasing from 40.88 $mg \cdot g^{-1}$ to 11.84 $mg \cdot g^{-1}$. This observation can be explained by the fact that increasing the bio adsorbent load

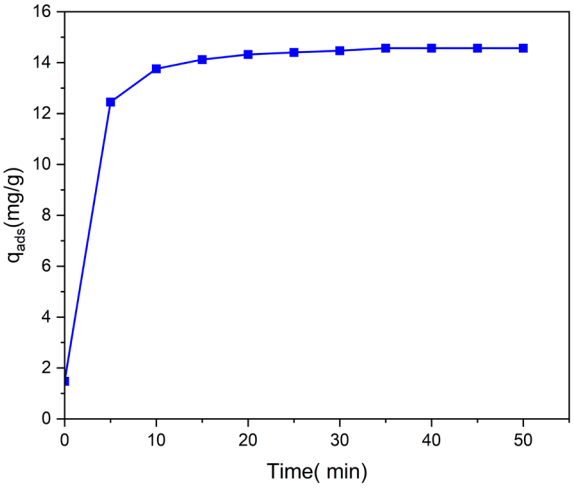

Fig. 5. Adsorption capacity of BM on DP as a function of contact time (pH = 5.6, T = 25°C, m_{ads} = 2g/l, [MB] = 30 mg/L, V = 200 ml).

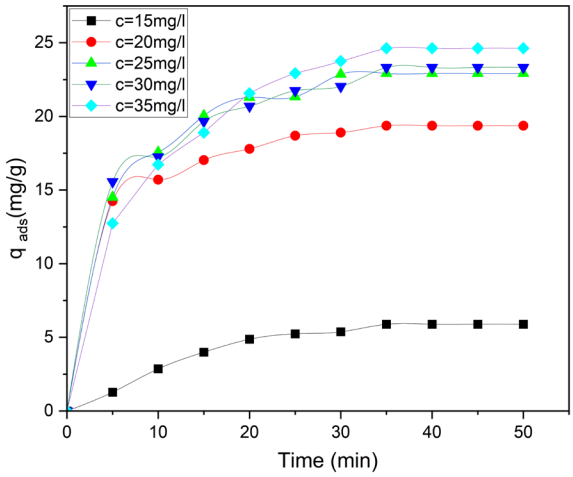

Fig. 6. Adsorption capacity of MB on DP as a function of initial MB concentration (t = 35 min, T = 25°C, pH = 5.6, m_{DP} = 1g/L, V = 200 ml)

increases the number of active adsorption sites (El Qada et al., 2006). Thus, the availability of adsorption sites contributes to enhancing the retention efficiency. Based on the intersection of the adsorption capacity and decolorization rate curves, it was determined that the optimal mass of bio adsorbent for improved adsorption in the removal of BM dyes is approximately 1.1 g. At this mass, a decolorization rate of approximately 77.5% is observed, with an adsorption efficiency of 21.5 mg·g^{-1}.

Effect of pH

To maximize contaminant adsorption by functional adsorbents, solution pH is a crucial parameter (Tor and Cengeloglu, 2006). Figure 9 illustrates the impact of pH on MB pollutant removal for a pH interval of 2 to 12. Date pits remove less dye at acidic pH levels for of the electromagnetic force among positively charge elements the bioadsorbent and the MB pollutant larger pH levels were observed to result in a larger percent (%) of dye removal by the bio adsorbent due to the electromagnetic attraction between the charge elements of the DP and the MB organic pollutant. larger pH levels were observed to result in a larger percent (%) of MB pollutant removal by DP due to the electromagnetic force between the charged molecules DP and the MB atoms (Senthilkumaar et al., 2005). The results in the figure below demonstrate that a basic environment is more favorable for dye adsorption on the studied material (DP) compared to an acidic environment. This can be attributed to the fact that the addition of H^+ protons neutralize the negative charge of the material, which hinders the adsorption of dyes in highly acidic environments and, conversely, favors it in basic environments.

Effect of temperature

In the 300–350 K° range, the effect of T (K°) on MB adsorption capability was studied. Figure 10 presents the impact of T (K°) on the dye retention rate on the adsorbent. From the figure, we observe that this rate decreases with increasing reactor temperature (Rahmani et al., 2010). According to this phenomenon and the Arrhenius equation, the surface reaction is exothermic, and each rise in temperature slows it down. The analysis of this figure shows that increasing the temperature leads to a slight decrease in adsorption capacity. The optimal adsorption occurs at room temperature.

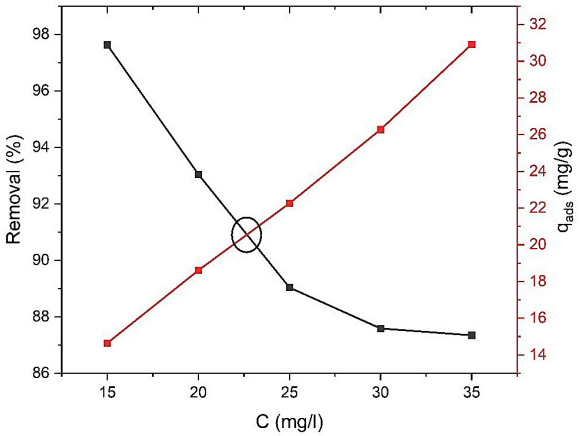

Fig. 7. Optimal MB concentration for adsorption with DP (t = 35 min, T = 25°C, pH = 5.6, m_{DP} = 2 g/L; V = 200 ml)

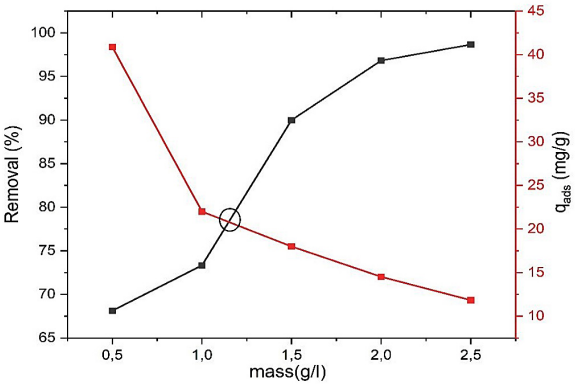

Fig. 8. Effect of m_{DP} on adsorption of MB (t = 35 min, T = 25°C, pH = 5.6, [MB] = 22.5 mg/L; v = 50 ml)

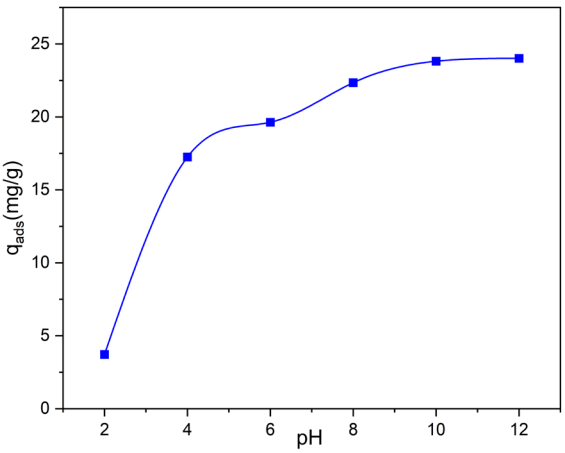

Fig. 9. Effect the pH of MB adsorption (t = 35 min, T = 25°C, [MB] = 22.5 mg/l, V = 50 ml, m_{DP} = 1.1g)

Effect of bioadsorbent size

Date pits (DP) that had been dried up and were still raw were broken up and sifted into various split sizes (250–355–500–700 um) to examine the effects of particle size on the adsorption process (Banat et al., 2003). Figure 11 demonstrates how the dye's adsorption ability declines as particle size rises. This is due to the fact that adsorption is reduced as particle size increases because of a reduction in specific surface area. It is possible to confirm that optimum adsorption is achieved at a particle size of 225 µm.

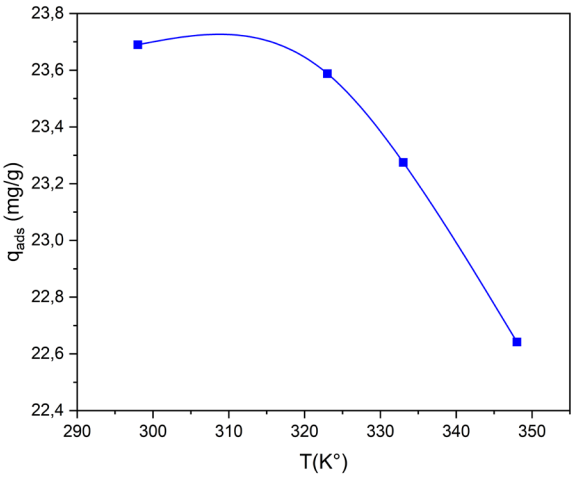

Fig. 10. Impact the T(K°) on adsorption of MB (t = 35 min, pHi = 5.6, [MB] = 22.5 mg/l, V = 50 ml, m_{DP} = 1.1 g).

ADSORPTION ISOTHERMS

Langmuir isotherms

The Freundlich, Langmuir and Dubin-Radushkevich models for the analysis of adsorption isotherms were reviewed and used to characterize the adsorption process for our research results. One of the theories for explaining monolayer adsorption is the Langmuir isotherm. It presupposes a homogenous adsorption surface with identically energetic binding sites. The following is how to express the Langmuir isotherm's linear form (Da, 2001):

$$\frac{1}{q_e} = \frac{1}{q_{max}} + \frac{1}{(K_L \times q_{max})} \times \frac{1}{C_e} \qquad (3)$$

The maximal adsorption capacity under experimental conditions is represented by q_{max} (mg/g), q_{max} and K_L are calculated from the plot of Ce / qe versus Ce.

The expression of the dimensionless parameter R_L, which represents the equilibrium or adsorption intensity, can be derived from further analysis of the Langmuir equation.

$$R_L = \frac{1}{1+K_L C_0} \qquad (4)$$

The R_L parameter, which is based on the initial amount of adsorbate (C_0) measured in mg/L, is considered a more reliable indicator of the adsorption process (Figure 12). The R_L value can be classified into four categories: (i) R_L between 0 and 1 indicates good adsorption, (ii) R_L above 1 indicates bad adsorption, (iii) R_L equal to 1

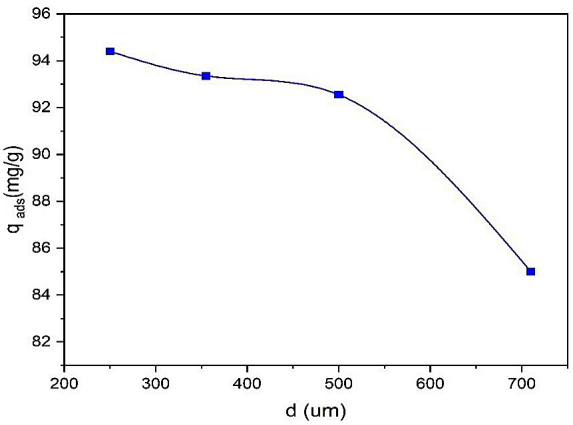

Fig. 11. Impact of particle size on MB adsorption on DP (t = 35 min, T = 25°C, pH = 5.6, [MB] = 22.5 mg/l, V = 50 ml, m_{DP} = 1.1 g)

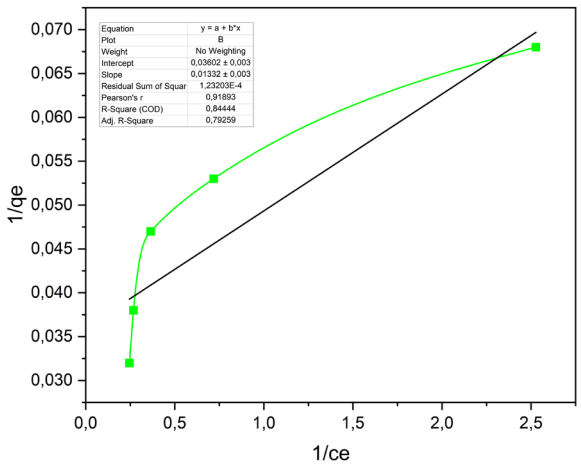

Fig. 12. Langmuir adsorption isotherm (t = 35 min, T = 25°C, PH = 5.6 [BM] = 22.5 mg/L, V = 200 ml, m_{DP} = 1.1 g).

represents linearly adsorption, and (iv) R_L equal to 0 means non-reversible adsorption (Angove et al., 1997).

Freundlich isotherm

The logarithmic equation applied to the investigation of the Freundlich isotherm (Fig. 13) is as follows (Boparai et al., 2011):

$$\text{Log}\,(q_e) = \log\,(k_F) + \frac{1}{n}\log(c_e) \qquad (5)$$

A curve with a slope of 1/n and an origin ordinate of Log (k_F) is obtained by transporting a log (q_e) as a function of *C*e. This allows us to calculate the constant K_F (mg/g) and the heterogeneity factor 1/n.

Dubinin-Radushkevich isotherm

In contrast to the Langmuir model, Dubinin-Radushkevich (Fig. 14) requires a homogenous surface. Its theory of micropore volume filling is predicated on the idea that the adsorption potential is changeable and that the adsorption free energy is correlated with the level of pore filling (Vijayaraghavan et al., 2006). The following equation results in the Dubinin-Radushkevich isotherm (Ayawei et al., 2015):

$$\ln(q_e) = \ln\,(q_m) - K_{DR}\,\varepsilon^2 \qquad (6)$$

where: q_m is the equilibrium adsorption capacity of DP (mg·g^{-1}),
K_{DR} presents the Dubinin-Radushkevich constant (mol^2·Kj^2), and
ε ($\varepsilon = RT \ln\,(1 + 1/C_e)$).

The average sorption energy (E) in kJ·mol^{-1} can be determined by utilizing the following equation (Saltalı et al., 2007).

$$E = \frac{1}{\sqrt{-2K_{DR}}} \qquad (7)$$

As far as applied models are concerned, both the Dubinin-Radushkevich and Langmuir adsorption models showed very low correlation coefficients for the experimental data, $R^2 = 0.70$, $R^2 = 0.83$, respectively. Table 2 demonstrates the inability of these models to accurately describe the

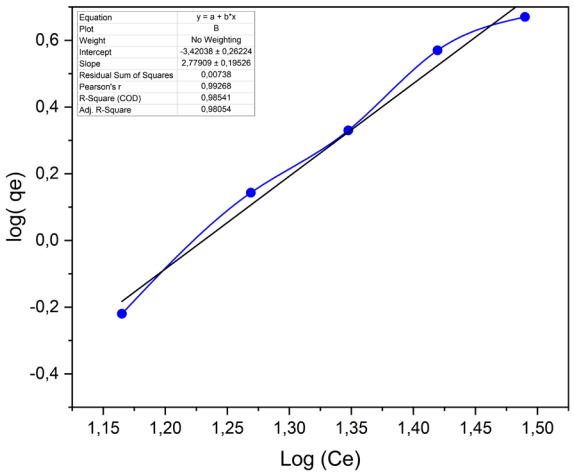

Fig. 13. Freundlich adsorption isotherm (t = 35 min, T = 25°C, PH = 5,6 [MB] = 22.5 mg/L, V = 200 ml, m_{DP} = 1.1 g)

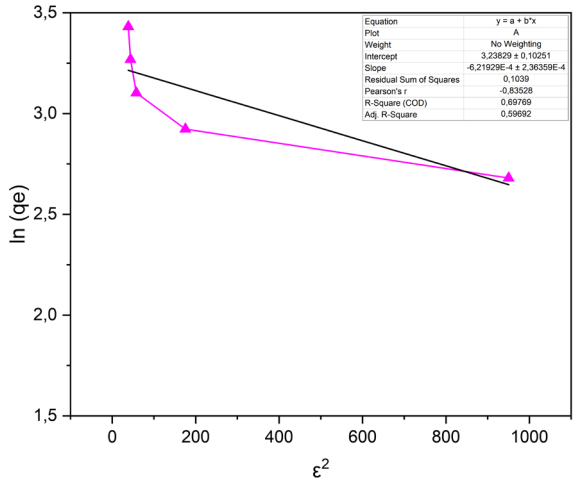

Fig. 14. Dubinin-Radushkevich adsorption isotherm (t = 35 min, T = 25°C, PH = 5.6, [MB] = 22.5 mg/L, V = 200 ml, m_{DP} = 1.1 g).

adsorption process of MB organic pollutant on the studied bioadsorbents. The inapplicability of the Dubinin-Radushkevich and Langmuir adsorption isotherms suggests that adsorption occurs on non-uniform adsorption sites due to the inequality of adsorption site activities on different date pit-based bioadsorbents. Correlation factor results presented in Table 2 demonstrate that the Freundlich model is the most appropriate for characterizing the adsorption of the organic pollutant MB on the bioadsorbent DP, as shown by the highest R^2 correlation coefficients.The parameter 1/n represents the relative distribution of energetic adsorption sites and depends on both the nature and intensity of the adsorption process. The obtained value for 1/n is typically less than 1, indicating

that the adsorption of MB organic pollutant on DP is favorable and corresponds to a chemical adsorption process.

Adsorption kinetics

The following equations define the kinetics of the pseudo-first-order and pseudo-second-order models, respectively (Fan et al., 2003):

$$Ln\ (qe\text{-}qt) = Ln\ (qe) - \frac{K1}{2.303}\ t \tag{8}$$

$$\frac{t}{q_t} = \frac{1}{K_2\ qe^2} + \frac{1}{qe}\ t \tag{9}$$

Plotting *Ln* (*qe* – *qt*) as a function of time (Fig. 14) results in a line with a slope of k_1 if the Lagergren connection is confirmed. A line with a slope of $1/q_e$ and a y-intercept of $1/k_2qe^2$ must be obtained in order to plot t/q_t as a function of time (Fig. 15). Table 3 shows that the pseudo-first-order model's equation is not linear and has a very low coefficient of correlation R^2, which shows that the experimental absorption capacity differs greatly from the value predicted by this model. Thus, we can deduce that the adsorption kinetics does not follow the pseudo-first-order model (Fig. 15). However, from the obtained results (Fig. 16, Table 3), it is evident that the variation of t/q_t with time is highly linear, and the regression coefficient R^2 is satisfactory. Thus, we can draw the conclusion that the kinetic adsorption of MB using date pits follows the pseudo-second-order model, which implies that the chemical interactions between dye molecules and the adsorbent surface are characterized by electron transfers (Krishnamoorthy et al., 2019).

Thermodynamic study

To understand the adsorption phenomenon better, knowledge of the thermodynamics of adsorption is essential (Fig. 17). Based on experimental data and the accompanying formulae, the Van't Hoff equations have been used to calculate the thermodynamic variables the adsorption process, including three variations such as: (ΔG°), (ΔH°), (ΔS°), Gibbs free energy, enthalpy, entropy (ΔS°), respectively (Singh and Pant, 2004),

Table 2. Adsorption isotherm parameters: Dubinin-Radushkevich (D-R), Freundlich, Langmuir

Module	Parameters	Value
Langmuir	q_{max} (mg/g)	27.39
	R_L	0.009
	K_L	2.74
	R^2	0.844
Freundlich	1/n	0.31
	K_F	0.001
	R^2	0.98
Dubinin-Radushkevich	E (kJ/mol)	9.12
	q_{max} (mg/g)	25.27
	K_{DR}	0.006
	R^2	0.69

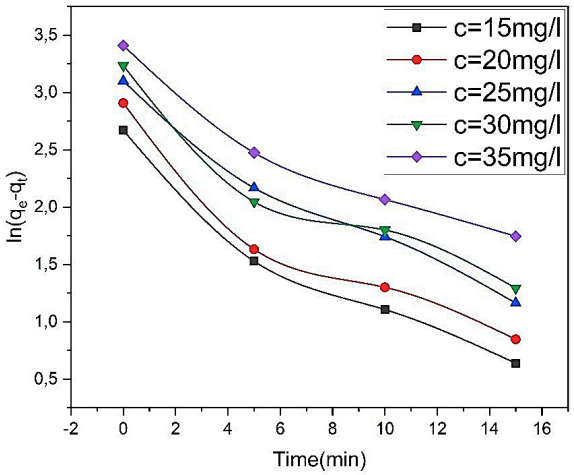

Fig. 15. Pseudo-first-order kinetics of MB adsorption on DP (t = 35 min, T = 25°C, pH = 5.6, [MB] = 22.5 mg/l, V = 50 ml, m_{DP} = 1.1 g)

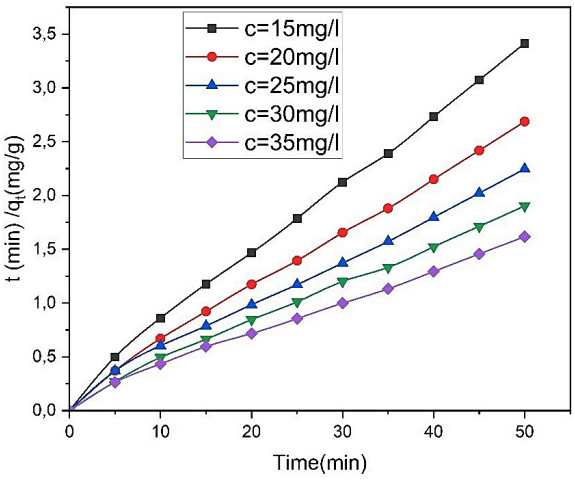

Fig. 16. Pseudo-second-order kinetics of MB adsorption on DP (t = 35 min, T = 25°C, pH = 5.6, [MB] = 22.5 mg/l, V = 50 ml, m_{DP} = 1.1 g)

Table 3. Parameters of kinetic models

		First order			Second order			
C_0 (mg/l)	q_{exp} (mg/g)	K_1 (min^{-1})	q_t (mg/g)	R^2	k_2 (g/mg·min)	q_t (mg/g)	R^2	
Dye (BM)	15	14.64	0.286	11.41	0.9626	0.031	15.24	0.997
	20	18.60	0.30	13.86	0.9038	0.027	19.30	0.997
	25	22.26	0.28	19.88	0.9733	0.016	23.52	0.995
	30	26.27	0.27	20	0.9073	0.015	27.39	0.996
	35	30.92	0.24	25.27	0.933	0.010	32.78	0.994

or ΔG° (kJ/mol), T (K),ΔH° (kJ/mol), R (J/mol. K), ΔS° (J/K) present the standard free energy,the absolute temperature,the universal constant,the standard entropy respectively.

The negative values of ΔG° at 298, 323, 333, and 348 degrees Celsius are displayed in Table 4 and illustrate that these temperatures enhance spontaneity of adsorption. At 298, 323, and 333 K, the adsorption of MB organic pollutant onto date pit cores followed a similar pattern. The negative standard enthalpy value, ΔH°, for MB signifies that the adsorption process is exothermic (Sari et al., 2007). The MB molecules are more structured at the solid-liquid interface than in the liquid phase, according to the negative entropy value, ΔS°. The adsorption process is spontaneous, according to the negative values of the free energy, ΔG°.

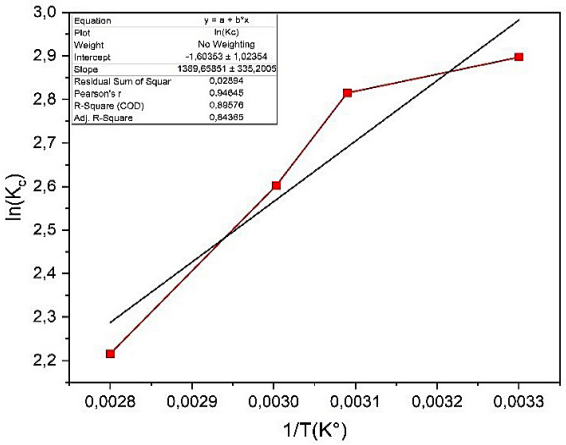

Fig. 17. Line of $\ln(K_C)$ versus 1/T for adsorption of MB on DP (t = 35 min, T = 25°C±4, pH = 5.6, [MB] = 22.5 mg/l, V = 50 ml, m_{DP}=1.1 g)

CONCLUSION

In the current study, we prepared an adsorbent for the batch system-based adsorption of MB organic pollutant from an aqueous solution using raw date pits, a cheap and easily accessible material. The findings revealed that an equilibrium reaction took 35 minutes to complete at a pH of 10, MB organic pollutant concentration of 22.5 $mg \cdot L^{-1}$, and an adsorbent mass of 1.1 $g \cdot L^{-1}$. The highest adsorption efficiency was at 24 $mg \cdot g^{-1}$. However, as temperature and particle size rose, the adsorption effectiveness fell off dramatically. Compared to other applicable isotherm models, the Freundlich isotherm model offered a superior fit for the adsorption process. The kinetic data of the MB adsorption process were closely associated with the pseudo-second-order model. The thermodynamic examination of adsorption yielded standard Gibbs free energy (ΔG°) and standard enthalpy (ΔH°) values, which show that the MB adsorption on date pits is exothermic and spontaneous. According to the study's findings, date pits are a highly effective adsorbent for removing colors from aqueous environments.

REFERENCES

1. Abdallah, M., Hijazi, A., Hamieh, M., Alameh, M., Toufaily, J., Rammal, H. 2016. Adsorption study of Methylene Blue on biomaterial using cactus. J. Mater. Environ. Sci. 7, 4036–4048.
2. Adachi, A., El Ouadrhiri, F., Kara, M., El Manssouri, I., Assouguem, A., Almutairi, M.H., Bayram, R., Mohamed, H.R.H., Peluso, I., Eloutassi, N., Lahkimi, A. 2022. Decolorization and degradation of

Table 4. Thermodynamic settings of the BM adsorption process on the bio adsorbent

ΔG° ($kJ \cdot mol^{-1}$)				ΔH° ($kJ \cdot mol^{-1}$)	ΔS° ($J \cdot mol^{-1} \cdot k^{-1}$)	R^2
T (K)						
298	323	333	348	-	-	-
-7.41	-7.11	-7.00	-6.82	-10.94	-11.83	0.77

methyl orange azo dye in aqueous solution by the electro fenton process: Application of optimization. Catalysts 12, 1–12. https://doi.org/10.3390/catal12060665

3. Adachi, A., Soujoud, R., El Ouadrhiri, F., Tarik, M., Hmamou, A., Eloutassi, N., Lahkimi, A. 2023. Cactus and holm oak acorn for efficient textile wastewater treatment by coagulation-flocculation process optimization using box-benhken design. J. Ecol. Eng. 24, 315–328. https://doi.org/10.12911/22998993/162784
4. Ahmad, A.Y., Al-Ghouti, M.A., Khraisheh, M., Zouari, N. 2022. Insights into the removal of lithium and molybdenum from groundwater by adsorption onto activated carbon, bentonite, roasted date pits, and modified-roasted date pits. Bioresour. Technol. Reports 18, 101045. https://doi.org/10.1016/j.biteb.2022.101045
5. Ahmad, M., Abbas, G., Haider, R., Jalal, F., Shar, G.A., Soomro, G.A., Qureshi, N., Iqbal, M., Nazir, A. 2019. Kinetics and equilibrium studies of Eriobotrya japonica: A novel adsorbent preparation for dyes sequestration. Zeitschrift fur Phys. Chemie 233, 1469–1484. https://doi.org/10.1515/zpch-2018–1201
6. Aisha MuthanaAlasadi1, F.I.A.M. 2019. Adsorption of Cu(II), Ni(II) and Zn(II) ions by nano kaolinite: Thermodynamics and kinetics studies. Chem. Int. ()- 5(), 258–268.
7. Ait Hmeid, H. 2021. Moroccan Journal of Chemistry Adsorption of a basic dye, Methylene Blue, in aqueous solution on bentonite DAOUDI (d). L. Mor. J. Chem 9, 416–433.
8. Al-Ghouti, M.A., Li, J., Salamh, Y., Al-Laqtah, N., Walker, G., Ahmad, M.N.M. 2010. Adsorption mechanisms of removing heavy metals and dyes from aqueous solution using date pits solid adsorbent. J. Hazard. Mater. 176, 510–520. https://doi.org/10.1016/j.jhazmat.2009.11.059
9. Alakhras, F., Alhajri, E., Haounati, R., Ouachtak, H., Addi, A.A., Saleh, T.A. 2020. A comparative study of photocatalytic degradation of Rhodamine B using natural-based zeolite composites. Surfaces and Interfaces 20, 100611. https://doi.org/10.1016/j.surfin.2020.100611
10. Ali, N.S., Jabbar, N.M., Alardhi, S.M., Majdi, H.S., Albayati, T.M. 2022. Adsorption of methyl violet dye onto a prepared bio-adsorbent from date seeds: isotherm, kinetics, and thermodynamic studies. Heliyon 8, e10276. https://doi.org/10.1016/j.heliyon.2022.e10276
11. Alipour, M., Vosoughi, M., Mokhtari, S.A., Sadeghi, H., Rashtbari, Y., Shirmardi, M., Azad, R. 2021. Optimising the basic violet 16 adsorption from aqueous solutions by magnetic graphene oxide using the response surface model based on the Box–Behnken design. Int. J. Environ. Anal. Chem. 101, 758–777. https://doi.org/10.1080/03067319.2019.1671378
12. Angove, M.J., Johnson, B.B., Wells, J.D., Box, P.O. 1997. SURFACES Adsorption of cadmium (II) on kaolinite 126, 137–147.
13. Arami, M., Limaee, N.Y., Mahmoodi, N.M., Tabrizi, N.S. 2005. Removal of dyes from colored textile wastewater by orange peel adsorbent: Equilibrium and kinetic studies. J. Colloid Interface Sci. 288, 371–376. https://doi.org/10.1016/j.jcis.2005.03.020
14. Awasthi, A., Jadhao, P., Kumari, K. 2019. Clay nano-adsorbent: structures, applications and mechanism for water treatment. SN Appl. Sci. 1, 1–21. https://doi.org/10.1007/s42452–019–0858–9
15. Ayawei, N., Ekubo, A.T., Wankasi, D., Dikio, E.D. 2015. Adsorption of Congo Red by Ni/Al-CO_3: Equilibrium, thermodynamic and kinetic studies. Oriental Journal of Chemistry 31(3), 1307-1318.
16. Banat, F., Al-Asheh, S., Al-Makhadmeh, L. 2003. Evaluation of the use of raw and activated date pits as potential adsorbents for dye containing waters. Process Biochem. 39, 193–202. https://doi.org/10.1016/S0032–9592(03)00065–7
17. Bayomie, O.S., Kandeel, H., Shoeib, T., Yang, H., Youssef, N., El-Sayed, M.M.H. 2020. Novel approach for effective removal of methylene blue dye from water using fava bean peel waste. Sci. Rep. 10, 1–10. https://doi.org/10.1038/s41598–020–64727–5
18. Boparai, H.K., Joseph, M., Carroll, D.M.O. 2011. Kinetics and thermodynamics of cadmium ion removal by adsorption onto nano zerovalent iron particles. J. Hazard. Mater. 186, 458–465. https://doi.org/10.1016/j.jhazmat.2010.11.029
19. Bouchelta, C., Medjram, M.S., Bertrand, O., Bellat, J.P. 2008. Preparation and characterization of activated carbon from date stones by physical activation with steam. J. Anal. Appl. Pyrolysis 82, 70–77. https://doi.org/10.1016/j.jaap.2007.12.009
20. Chakma, S., Moholkar, V.S. 2016. Synthesis of bimetallic oxides nanotubes for fast removal of dye using adsorption and sonocatalysis process. J. Ind. Eng. Chem. 37, 84–89. https://doi.org/10.1016/j.jiec.2016.03.009
21. Dąbrowski A. 2001. Adsorption – from theory to practice. Advances in Colloid and Interface Science 93(1–3), 135-224.
22. Diarra, M. 2019. Etude Cinetique De La Photodegradation Du Colorant Red 6 En Solution Aqueuse. Int. J. Adv. Res. 7, 124–130. https://doi.org/10.21474/ijar01/9638
23. Douara, N., Bestani, B., Benderdouche, N., Duclaux, L. 2016. Sawdust-based activated carbon ability in the removal of phenol-based organics from aqueous media. Desalin. Water Treat. 57, 5529–5545. https://doi.org/10.1080/19443994.2015.1005151

24. Dra, A., El Gaidoumi, A., Tanji, K., Chaouni Benabdallah, A., Taleb, A., Kherbeche, A. 2019. Characterization and quantification of heavy metals in oued sebou sediments. Sci. World J. 2019. https://doi.org/10.1155/2019/7496576
25. Dutta, A. 2017. Fourier transform infrared spectroscopy. In: Spectroscopic Methods for Nanomaterials Charaterization. Elsevier Inc. pp. 73–93. https://doi.org/10.1016/B978–0-323–46140–5.00004–2
26. El Ouadrhiri, F., Abdu Musad Saleh, E., Husain, K., Adachi, A., Hmamou, A., Hassan, I., Mostafa Moharam, M., Lahkimi, A. 2023. Acid assisted-hydrothermal carbonization of solid waste from essential oils industry: Optimization using I-optimal experimental design and removal dye application. Arab. J. Chem. 16. https://doi.org/10.1016/j.arabjc.2023.104872
27. El Qada, E.N., Allen, S.J., Walker, G.M. 2006. Adsorption of basic dyes onto activated carbon using microcolumns. Ind. Eng. Chem. Res. 45, 6044–6049. https://doi.org/10.1021/ie060289e
28. Fan, X., Parker, D.J., Smith, M.D. 2003. Adsorption kinetics of fluoride on low cost materials 37, 4929–4937. https://doi.org/10.1016/j.watres.2003.08.014
29. Gómez, V., Larrechi, M.S., Callao, M.P. 2007. Kinetic and adsorption study of acid dye removal using activated carbon. Chemosphere 69, 1151–1158. https://doi.org/10.1016/j.chemosphere.2007.03.076
30. Hassan, S.S., Al-Ghouti, M.A., Abu-Dieyeh, M., McKay, G. 2020. Novel bioadsorbents based on date pits for organophosphorus pesticide remediation from water. J. Environ. Chem. Eng. 8, 103593. https://doi.org/10.1016/j.jece.2019.103593
31. Javid, N., Malakootian, M. 2017. Removal of bisphenol a from aqueous solutions by modified-carbonized date pits by zno nano-particles. Desalin. Water Treat. 95, 144–151. https://doi.org/10.5004/dwt.2017.21592
32. Javid, N., Nasiri, A., Malakootian, M. 2019. Removal of nonylphenol from aqueous solutions using carbonized date pits modified with ZnO nanoparticles. Desalin. Water Treat. 141, 140–148. https://doi.org/10.5004/dwt.2019.23428
33. Krishnamoorthy, R., Govindan, B., Banat, F., Sagadevan, V., Purushothaman, M., Show, P.L. 2019. Date pits activated carbon for divalent lead ions removal. J. Biosci. Bioeng. 128, 88–97. https://doi.org/10.1016/j.jbiosc.2018.12.011
34. Ledakowicz, S., Solecka, M., Zylla, R. 2001. Biodegradation, decolourisation and detoxification of textile wastewater enhanced by advanced oxidation processes. J. Biotechnol. 89, 175–184. https://doi.org/10.1016/S0168–1656(01)00296–6
35. Li, J., Hu, J., Sheng, G., Zhao, G., Huang, Q. 2009. Colloids and Surfaces A : Physicochemical and engineering aspects effect of pH, ionic strength, foreign ions and temperature on the adsorption of Cu (II) from aqueous solution to GMZ bentonite. Colloids and Surfaces A: Physicochemical and Engineering Aspects 349, 195–201. https://doi.org/10.1016/j.colsurfa.2009.08.018
36. Miyah, Y., Idrissi, M., Zerrouq, F. 2015. Study and modeling of the kinetics methylene blue adsorption on the clay adsorbents (Pyrophillite, Calcite). J. Mater. Environ. Sci. 6, 699–712.
37. Narasimharao, K., Al-Thabaiti, S., Rajor, H.K., Mokhtar, M., Alsheshri, A., Alfaifi, S.Y., Siddiqui, S.I., Abdulla, N.K. 2022. Fe3O4@date seeds powder: A sustainable nanocomposite material for wastewater treatment. J. Mater. Res. Technol. 18, 3581–3597. https://doi.org/10.1016/j.jmrt.2022.03.176
38. Ouachtak, H., Akhouairi, S., Haounati, R., Addi, A.A., Jada, A., Taha, M.L., Douch, J. 2020. 3,4-dihydroxybenzoic acid removal from water by goethite modified natural sand column fixed-bed: Experimental study and mathematical modeling. Desalin. Water Treat. 194, 439–449. https://doi.org/10.5004/dwt.2020.25562
39. Pal, D.B., Singh, A., Jha, J.M., Srivastava, N., Hashem, A., Alakeel, M.A., Abd_Allah, E.F., Gupta, V.K. 2021. Low-cost biochar adsorbents prepared from date and delonix regia seeds for heavy metal sorption. Bioresour. Technol. 339, 125606. https://doi.org/10.1016/j.biortech.2021.125606
40. Pandian, C.J., Palanivel, R., Dhananasekaran, S. 2015. Chinese Journal of Chemical Engineering Green synthesis of nickel nanoparticles using Ocimum sanctum and their application in dye and pollutant adsorption. CJCHE 23, 1307–1315. https://doi.org/10.1016/j.cjche.2015.05.012
41. Rahman, M.S., Kasapis, S., Al-Kharusi, N.S.Z., Al-Marhubi, I.M., Khan, A.J. 2007. Composition characterisation and thermal transition of date pits powders. J. Food Eng. 80, 1–10. https://doi.org/10.1016/j.jfoodeng.2006.04.030
42. Rahmani, A., Mousavi, H.Z., Fazli, M. 2010. Effect of nanostructure alumina on adsorption of heavy metals. Desalination 253, 94–100. https://doi.org/10.1016/j.desal.2009.11.027
43. Saad, E.M., Mansour, R.A., El-Asmy, A., El-Shahawi, M.S. 2008. Sorption profile and chromatographic separation of uranium (VI) ions from aqueous solutions onto date pits solid sorbent. Talanta 76, 1041–1046. https://doi.org/10.1016/j.talanta.2008.04.065
44. Saltalı, K., Sarı, A., Aydın, M. 2007. Removal of ammonium ion from aqueous solution by natural Turkish (Yıldızeli) zeolite for environmental quality. Journal of Hazardous Materials 141(6), 258–263. https://doi.org/10.1016/j.jhazmat.2006.06.124
45. Sari, A., Tuzen, M., Citak, D., Soylak, M. 2007. Equilibrium, kinetic and thermodynamic studies

of adsorption of Pb (II) from aqueous solution onto Turkish kaolinite clay. Journal of Hazardous Materials 149, 283–291. https://doi.org/10.1016/j.jhazmat.2007.03.078

46. Senthilkumaar, S., Varadarajan, P.R., Porkodi, K., Subbhuraam, C.V. 2005. Adsorption of methylene blue onto jute fiber carbon: Kinetics and equilibrium studies. Journal of Colloid and Interface Science 284, 78–82. https://doi.org/10.1016/j.jcis.2004.09.027
47. Shan, R. ran, Yan, L. guo, Yang, Y. ming, Yang, K., Yu, S. jun, Yu, H. qin, Zhu, B. cun, Du, B. 2015. Highly efficient removal of three red dyes by adsorption onto Mg-Al-layered double hydroxide. J. Ind. Eng. Chem. 21, 561–568. https://doi.org/10.1016/j.jiec.2014.03.019
48. Singh, T.S., Pant, K.K. 2004. Equilibrium, kinetics and thermodynamic studies for adsorption of As (III) on activated alumina. Separation and Purification Technology 36, 139–147. https://doi.org/10.1016/S1383–5866(03)00209–0
49. Soares, O.S.G.P., Órfão, J.J.M., Portela, D., Vieira, A., Pereira, M.F.R. 2006. Ozonation of textile effluents and dye solutions under continuous operation: Influence of operating parameters. J. Hazard. Mater. 137, 1664–1673. https://doi.org/10.1016/j.jhazmat.2006.05.006
50. Susanti, R.F., Arie, A.A., Kristianto, H., Erico, M., Kevin, G., Devianto, H. 2019. Activated carbon from citric acid catalyzed hydrothermal carbonization and chemical activation of salacca peel as potential electrode for lithium ion capacitor's cathode. Ionics (Kiel). 25, 3915–3925. https://doi.org/10.1007/s11581–019–02904-x
51. Tan, K.B., Vakili, M., Horri, B.A., Poh, P.E., Abdullah, A.Z., Salamatinia, B. 2015. Adsorption of dyes by nanomaterials: Recent developments and adsorption mechanisms. Sep. Purif. Technol. 150, 229–242. https://doi.org/10.1016/j.seppur.2015.07.009
52. Tor, A., Cengeloglu, Y. 2006. Removal of congo red from aqueous solution by adsorption onto acid activated red mud. J. Hazard. Mater. 138, 409–415. https://doi.org/10.1016/j.jhazmat.2006.04.063
53. Vijayaraghavan, K., Padmesh, T.V.N., Palanivelu, K., Velan, M. 2006. Biosorption of nickel (II) ions onto Sargassum wightii : Application of two-parameter and three-parameter isotherm models 133, 304–308. https://doi.org/10.1016/j.jhazmat.2005.10.016
54. Wang, H., Gong, G., Zhou, H., Wang, W. 2016. Steady flow torques in a servo motor operated rotary directional control valve. Energy Convers. Manag. 112, 1–10. https://doi.org/10.1016/j.enconman.2015.11.054
55. Xing, J., Huang, J., Wang, X., Yang, F., Bai, Y., Li, S., Zhang, X. 2023. Removal of low-concentration tetracycline from water by a two-step process of adsorption enrichment and photocatalytic regeneration. J. Environ. Manage. 343, 118210. https://doi.org/10.1016/j.jenvman.2023.118210
56. Gui Chen Y., Min Ye W., Min Yang X., Yue Deng F., He Y. 2011. Effect of contact time, pH, and ionic strength on Cd(II) adsorption from aqueous solution onto bentonite from Gaomiaozi, China. Environmental Earth Sciences 64, 329–336. https://doi.org/10.1007/s12665–010–0850–6
57. Yuvaraja, G., Zheng, N.C., Pang, Y., Su, M., Chen, D.Y., Kong, L.J., Mehmood, S., Subbaiah, M.V., Wen, J.C. 2020. Removal of U(VI) from aqueous and polluted water solutions using magnetic Arachis hypogaea leaves powder impregnated into chitosan macromolecule. Int. J. Biol. Macromol. 148, 887–897. https://doi.org/10.1016/j.ijbiomac.2020.01.042
58. Zhang, Z., Wang, W., Kang, Y., Zong, L., Wang, A. 2016. Tailoring the properties of palygorskite by various organic acids via a one-pot hydrothermal process: A comparative study for removal of toxic dyes. Appl. Clay Sci. 120, 28–39. https://doi.org/10.1016/j.clay.2015.11.019
59. Zhou, F., Cheng, Y., Gan, L., Chen, Z., Megharaj, M., Naidu, R. 2014. Burkholderia vietnamiensis C09V as the functional biomaterial used to remove crystal violet and Cu(II). Ecotoxicol. Environ. Saf. 105, 1–6. https://doi.org/10.1016/j.ecoenv.2014.03.028